Cubic Phases in Phosphatidylcholine-Cholesterol Mixtures: Cholesterol as Membrane ''Fusogen''

Boris G. Tenchov,* Robert C. MacDonald,* and David P. Siegel†
*Northwestern University, Department of Biochemistry, Molecular Biology and Cell Biology, Evanston, Illinois; and †Givaudan Inc., Cincinnati, Ohio

ABSTRACT X-ray diffraction reveals that mixtures of some unsaturated phosphatidylcholines (PCs) with cholesterol (Chol) readily form inverted bicontinuous cubic phases that are stable under physiological conditions. This effect was studied in most detail for dioleoyl PC/Chol mixtures with molar ratios of 1:1 and 3:7. Facile formation of Im3m and Pn3m phases with lattice constants of 30–50 nm and 25–30 nm, respectively, took place in phosphate-buffered saline, in sucrose solution, and in water near the temperature of the L_α–H_{II} transition of the mixtures, as well as during cooling of the H_{II} phase. Once formed, the cubic phases displayed an ability to supercool and replace the initial L_α phase over a broad range of physiological temperatures. Conversion into stable cubic phases was also observed for mixtures of Chol with dilinoleoyl PC but not for mixtures with palmitoyl-linoleoyl PC or palmitoyl-oleoyl PC, for which only transient cubic traces were recorded at elevated temperatures. A saturated, branched-chain PC, diphytanoyl PC, also displayed a cubic phase in mixture with Chol. Unlike the PEs, the membrane PCs are intrinsically nonfusogenic lipids: in excess water they only form lamellar phases and not any of the inverted phases on their own. Thus, the finding that Chol induces cubic phases in mixtures with unsaturated PCs may have important implications for its role in fusion. In ternary mixtures, saturated PCs and sphingomyelin are known to separate into liquid-ordered domains along with Chol. Our results thus suggest that unsaturated PCs, which are excluded from these domains, could form fusogenic domains with Chol. Such a dual role of Chol may explain the seemingly paradoxical ability of cell membranes to simultaneously form rigid, low-curvature raft-like patches while still being able to undergo facile membrane fusion.

INTRODUCTION

Because cholesterol (Chol) is a major component of animal cell membranes, the structure and phase behavior of a variety of Chol-phospholipid mixtures have been subject of keen interest and numerous studies in the past 40 years (1–4). It is generally believed that Chol plays key role in the membrane lateral organization. Chol is known to interact preferentially with other membrane lipid components, specifically, the phosphatidylcholines (PC) and sphingomyelin (SM), thereby increasing the degree of chain order and promoting formation of domains of so called liquid-ordered phase (L_o), in which lipid diffusion is slower than in the liquid-crystalline L_α phase. It has been demonstrated for ternary mixtures of Chol with PCs and SM that PCs with saturated chains and SM tend to associate with Chol in domains of L_o phase, whereas PCs with unsaturated chains tend to be excluded and to form liquid-disordered phase (L_d) (5–10). On basis of studies on model systems and on detergent-resistant domains in biomembrane extracts, it has been suggested that domains of the L_o phase may also form in the membranes of eukaryotic cells. Such domains, referred to as ''rafts'', may serve as sites for specific lipid-protein interactions regulating the activities of certain membrane proteins (see, e.g., various reviews (11–13)).

Studies on enveloped viruses (Semliki Forest virus, Sindbis virus, HIV, influenza virus) have established that their fusion with cells requires or is accelerated by the presence of Chol and sphingolipids in the host or viral membranes (14–26). Notably, Chol is also necessary for rapid and efficient membrane fusion in the sea urchin cortical granule/plasma membrane system (27). As noted above, the latter lipids can form liquid-ordered domains in the presence of PCs; however, no evidence has been found that such domains (rafts) play any role in the process of virus entry (16,24,28). On the other hand, it is known that Chol also serves as a source of negative curvature in the lipid bilayers (29). Studies by Epand et al. (30–32) have shown that mixtures of unsaturated PCs with Chol are capable of forming an inverted hexagonal phase, H_{II}, at elevated temperatures. Isotropic ^{31}P NMR patterns have also been observed; however, no x-ray diffraction patterns indicating formation of inverted cubic phases have been found (30–32).

In this work, we used x-ray diffraction to demonstrate that mixtures of Chol with some unsaturated PCs can readily form inverted bicontinuous cubic phases, which are stable under physiological conditions. The properties of the cubic phases in PC/Chol mixtures closely resemble those observed earlier for cubic phases induced in phosphatidylethanolamine (PE) dispersions (33). These results suggest that unsaturated PCs, which are excluded from the liquid-ordered domains, could form fusogenic domains with Chol. Such a dual effect of Chol may explain the seemingly paradoxical ability of cell membranes to simultaneously form rigid,

Submitted February 22, 2006, and accepted for publication June 23, 2006.

Address reprint requests to B. Tenchov, Northwestern University, Dept. of Biochemistry, Molecular Biology and Cell Biology, Evanston, IL 60208. E-mail: b-tenchov@northwestern.edu.

0006-3495/06/10/2508/09 $2.00

doi: 10.1529/biophysj.106.083766

low-curvature raft-like patches while still being able to undergo facile membrane fusion. A preliminary account of this work has appeared elsewhere (34).

MATERIALS AND METHODS

Sample preparation

The phospholipids, DOPC (1,2-dioleoyl-*sn*-glycero-3-phosphocholine), POPC (1-palmitoyl-2-oleoyl-*sn*-glycero-3-phosphocholine), palmitoyl-linoleoyl PC (1-palmitoyl-2-linoleoyl-*sn*-glycero-3-phosphocholine), and dilinoleoyl PC (1,2-linoleoyl-*sn*-glycero-3-phosphocholine) (Avanti Polar Lipids, Alabaster, AL) were checked for purity by mass spectroscopy (DOPC only) and TLC and found to contain no detectable admixtures. Cholesterol (Sigma, standard for chromatography) was >99% pure. Appropriate PC and Chol amounts were codissolved in chloroform, the chloroform was removed with a stream of argon, and the mixtures were subjected to high vacuum for 18–24 h. Lipid dispersions were prepared by hydrating and vortexing at room temperature, followed by five freeze-thaw cycles between dry ice and room temperature, accompanied by vortexing during the thawing steps. Most measurements were carried out on dispersions with lipid contents of 10% (w/v). Dispersions with lipid contents of 30% and 50% (w/v) were also used, as indicated under Results. The dispersion media used were 320 mM sucrose, PBS and ×10 PBS solutions, and also water. The ×10 PBS buffer (pH 6.7–6.9) was Dulbecco's Phosphate-Buffered Saline (PBS, Gibco). PBS (pH 7.1 ± 0.1) was prepared by diluting ×10 PBS 10 times. The dispersions were stored at 4°C, typically for ~1 day, and equilibrated at room temperature for several hours before the x-ray measurements. The samples were vortexed again, loaded into x-ray capillaries, and flame sealed immediately before their measurement. Temperature protocols were executed directly on samples mounted on the beam line, and it was possible to follow in real time the conversion of these dispersions into cubic phase. Because we typically used relatively high scan rates of 3–10°C/min in this study, the L_α–H_{II} phase transition temperatures recorded may be higher than the equilibrium transition midpoints, which may only be obtained using very low, quasistatic scan rates (see, e.g., Toombes et al. (35)). This circumstance, however, does not affect in any substantive way the conclusions derived from the x-ray data with regard to the process of formation and the properties of the bilayer cubic phases. The high scan rates used reduced the exposures of the samples to elevated temperatures and, consequently, minimized the potential for formation of lipid degradation products. Lipids extracted from the hydrated samples after the measurements were found to give single TLC spots identical to those for lipids extracted from unused dispersions. It is noteworthy that no evidence for lipid degradation has been found in DSC studies of DOPC/Chol mixtures, which, because of the low DSC scan rates, were exposed to high temperatures for longer times than were x-ray samples (30; our unpublished DSC data). In summary, we conclude that neither the heating-cooling protocols nor the constant-temperature incubations used in our work resulted in noticeable lipid degradation.

X-ray measurements

Low-angle x-ray patterns were recorded at stations 18D, BioCAT, and 5IDD, DND-CAT, APS, Argonne, using 2-D 2048 × 2048 MAR detectors at a sample-to-detector distance of ~200 cm. Spacings were determined from axially integrated 2-D images using the FIT2D program and silver behenate as calibration standard. A temperature-controlled (Linkam thermal stage) capillary sample holder was used. All measurements were started at 20°C. The sample holder was mounted on a motorized stage, and, by moving it with respect to the incident beam, it was possible to ensure that the patterns recorded were representative of the whole sample volumes.

Radiation damage controls

The exposure times used for collection of x-ray diffraction patterns were in the range of 0.7–1 s. As can be seen from Figs. 1 and 2, we usually recorded ~10–15 x-ray patterns to follow the conversion into cubic phase and a total of ~20–25 patterns throughout an experiment. In this way, the irradiation times during the cubic phase formation were typically limited to 10–15 s, and total irradiation times were typically limited to 20–25 s. These times are several times shorter than the exposure times of a few minutes needed to cause observable radiation damage in lipid dispersions under our experimental conditions. As noted above, no degradation products were detected by TLC of lipids extracted from the dispersions after the experiments. However, it should be recognized that these tests are not sensitive in detecting radiation damage because with a beam cross-section of ~150 × 150 μm, the irradiated dispersion volume usually represents less than 1% of the total sample volume in the capillary.

We used the following checks for eventual artifacts caused by lipid molecules damaged by radiation. By moving the sample holder with respect to the incident x-ray beam, it was possible to record and compare x-ray patterns from irradiated and several nonirradiated parts of the sample. Such comparisons were made throughout the experiments, and they revealed no systematic differences between irradiated and nonirradiated sample portions within the exposure time limits described above. We noticed, however, that longer exposure times initially resulted in x-ray patterns with broadened reflections relative to patterns recorded from neighboring nonirradiated sample portions. We did not investigate this effect in detail, although it appears to indicate the onset of radiation damage in these dispersions. Also, we made measurements with ''dark'' samples subjected to identical temperature protocols but with only three or four x-ray patterns being recorded in the course of the experiment with the purpose of verifying the state of the dispersion. Such samples were found to reach final states that were virtually identical to those of the irradiated samples. On the basis of these tests, we

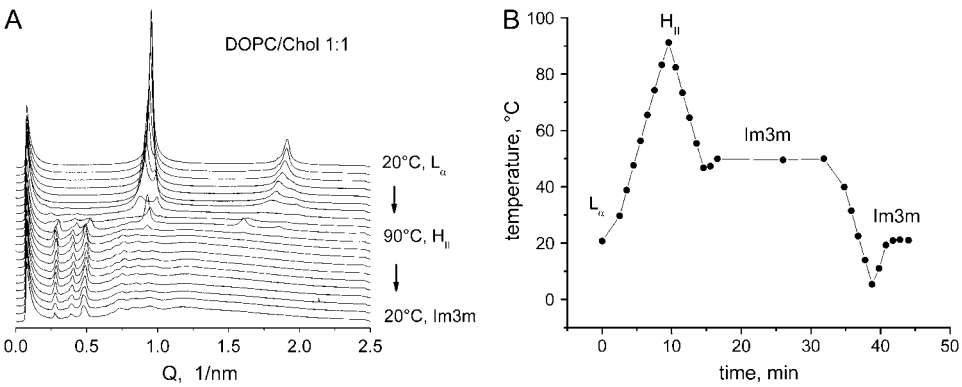

FIGURE 1 (*A*) Sequence of x-ray diffraction patterns showing a lamellar-to-cubic phase conversion ($L_\alpha \rightarrow$ Im3m) in DOPC/Chol 1:1 mixture, 10% (w/v) in PBS, during a heating-cooling cycle. The initial L_α and final Im3m patterns are shown in Fig. 3, *A* and *B*, respectively. (*B*) Temperature protocol for the $L_\alpha \rightarrow$ Im3m conversion in *A*.

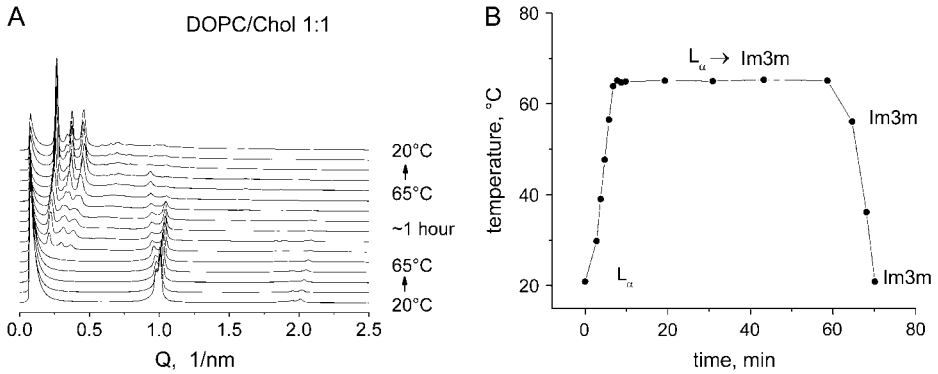

FIGURE 2 (*A*) Sequence of x-ray diffraction patterns showing a lamellar-to-cubic phase conversion ($L_\alpha \rightarrow$ Im3m) in DOPC/Chol 1:1 mixture, 10% (w/v) in ×10 PBS, on incubation at 65°C, followed by cooling to 20°C. (*B*) Temperature protocol for the $L_\alpha \rightarrow$ Im3m conversion in *A*.

conclude that the results reported here were not influenced by radiation damage to the lipid.

RESULTS

Here we show that mixtures of Chol with two unsaturated phosphatidylcholines, DOPC and dilinoleoyl PC, readily form stable inverted bicontinuous cubic phases. In these mixtures, conversions of the initial lamellar into cubic phase took place only at elevated temperatures, near the L_α–H_{II} phase transitions, or on cooling from the H_{II} phase. Once formed, the cubic phases were long-lived, able to supercool and to replace the initial L_α phase over the whole tested range (>0°C) of its existence. The process of cubic phase formation was studied in most detail for DOPC/Chol mixtures with molar ratios of 1:1 and 3:7. Conversion into stable cubic phase was also recorded for mixtures of Chol with dilinoleoyl PC but not for mixtures with POPC and palmitoyllinoleoyl PC. The latter two mixtures only exhibited transient traces of cubic phases at high temperatures. A saturated, branched-chain PC, diphytanoyl PC, also displayed a cubic phase in a 1:1 mixture with Chol.

We used lipid contents of 10% (w/v), which are relatively low for x-ray studies, to eliminate restricted volume effects and to ensure sufficiently large aqueous spaces in the lipid dispersions for cubic phases to develop. As shown in previous research, the use of dilute dispersions is an essential prerequisite for rapid formation of bicontinuous cubic phases in membrane lipid dispersions (33). We also used a freeze-thaw procedure for preparation of the dispersions to eliminate eventual irreversible effects of higher temperatures. In this way, it was possible to compare the initial lamellar state of dispersions that had not been heated above room temperature with their states after heating to the range of the H_{II} phase and subsequent cooling.

Temperature protocols for conversion of PC/Chol mixtures into cubic phase

The temperature protocols for inducing cubic phases in PC/Chol mixtures were similar to those developed earlier for accelerated formation of cubic phases in phosphatidylethanolamine (PE) dispersions (33,36). Generally, cubic phase formation proceeds at the highest rate when the dispersion is cooled from its H_{II} range and at temperatures that are roughly within the hysteresis loop of the L_α–H_{II} phase transition, i.e., between the temperatures of the cooling $H_{II} \rightarrow L_\alpha$ and heating $L_\alpha \rightarrow H_{II}$ transitions. At Chol molar fractions >0.6, DOPC/Chol mixtures display L_α–H_{II} transitions at temperatures above ~65–70°C (30). We therefore applied protocols involving heating at rates of 3–10°/min from the initial L_α state at 20°C into the H_{II} range of the mixtures. Once the H_{II} phase replaced the L_α phase according to the x-ray patterns, heating was terminated, and the dispersion was cooled to the L_α temperature range, either to an intermediate temperature, e.g., ~50°C or directly back to 20°C. Typically, the highest temperatures reached were 5–10°C above the $L_\alpha \rightarrow H_{II}$ transition onset, which was at ~75–80°C in our DOPC/Chol 1:1 dispersions in PBS. In all DOPC/Chol samples studied, cubic phase traces became visible in the patterns before or along with formation of the H_{II} phase. During the cooling step, these traces rapidly developed into well-ordered cubic phases. With the disappearance of the H_{II} phase at ~70°C, the dispersions were always either fully or over 90% converted into cubic phase (Fig. 1). Occasionally small peaks appeared in the patterns, resulting from partial recovery of the L_α phase. The heights of these peaks were several percent of those of the initial L_α phase. A second heating-cooling cycle was sufficient to abolish the residual L_α phase in these cases. That one or two temperature cycles were sufficient for conversion of the L_α phase into cubic phase shows that the formation of cubic phases in diluted DOPC/Chol mixtures is a very facile process in comparison to the previously studied PE dispersions, which typically require 10–15 or more cycles for full conversion, e.g., ~20 cycles at 10°C/min for dielaidoyl PE dispersions (33). Scan rate variations in the temperature protocol and short incubations in the H_{II} phase range were not found to have any noteworthy effects on the cubic phase formation and properties.

An alternative temperature protocol for cubic phase formation is an isothermal incubation of lipid dispersions at temperatures just below the onset of the $L_\alpha \rightarrow H_{II}$ transition.

Such a protocol was used previously for induction of cubic phase in monomethylated dioleoyl PE (DOPE-Me) dispersions (37). To test this protocol, in some experiments the heating was terminated and the dispersion incubated at a constant temperature a few degrees below the temperature of the expected appearance of the H_{II} phase. These experiments indicated that cubic phase formation in DOPC/Chol mixtures can also take place directly from the L_α phase. An example of such isothermal conversion, which, at least initially, proceeds without detectable involvement of the H_{II} phase, is given in Fig. 2. However, a small amount of H_{II} phase starts to form later, as evidenced by the appearance of a peak corresponding to the H_{II} $1/\sqrt{3}$ reflection (not visible in Fig. 2). Although it is conceivable that the incubation temperature could be lowered to values where no H_{II} phase would be expected to form, our experience with PC/Chol mixtures suggests that lowering the incubation temperature to such values results in a large increase of the conversion times, to the order of days, thus making the ''incubation'' protocol for direct L_α-to-cubic conversions impractical in real-time x-ray measurements.

Cubic phases in different PC/Chol mixtures: Role of the PC acyl chain composition

Representative examples of cubic phase patterns induced by the temperature protocols described above are shown in Figs. 3 and 4 *A*. All patterns shown were recorded at 20°C to illustrate the ability of the cubic phases to supercool and replace the initial lamellar phase at physiological temperatures. On storage of cubic phase dispersions for up to 6–10 h (~24 h in a single experiment) at room temperature, their diffraction patterns did not change, and no L_α phase reappeared. On these grounds, we regard the induced cubic phases to be sufficiently long-lived and stable in physiological conditions, although, strictly speaking, they should be probably termed metastable with respect to the lamellar phase at room temperatures. The typical ''final'' cubic phase in 10% (w/v) DOPC/Chol mixtures can be assigned as a pure or dominant Im3m cubic phase accompanied by a small contribution of the Pn3m cubic phase. The Im3m patterns comprised three prominent reflections in ratios of $\sqrt{2}$:$\sqrt{4}$:$\sqrt{6}$ and several smaller reflections in ratios of $\sqrt{8}$:$\sqrt{10}$:$\sqrt{12}$:$\sqrt{14}$:$\sqrt{16}$:$\sqrt{18}$:$\sqrt{20}$:$\sqrt{22}$. Such a reflection set is consistent with cubic aspect 8, extinction symbol I- - -; space group of highest symmetry Im3m (Q^{229}) (38). The reflection $\sqrt{8}$ was typically absent or very weak in these patterns. The Pn3m patterns (e.g., Fig. 4 *A*) comprise reflections in ratios $\sqrt{2}$:$\sqrt{3}$:$\sqrt{4}$:$\sqrt{6}$:$\sqrt{8}$:$\sqrt{9}$:$\sqrt{10}$:$\sqrt{11}$:$\sqrt{12}$:$\sqrt{14}$, consistent with cubic aspect 4 (space groups Pn3m/Pn3) (38). The lattice constant ratios of coexisting Im3m and Pn3m phases were always equal to 1.28 (Fig. 3 *C*), as has been the case for Im3m/Pn3m mixtures formed in PE dispersions (33). For 10% (w/v) DOPC/Chol 1:1 and 3:7 mixtures, cubic phases were readily forming in all three solutions used (PBS, ×10 PBS, and 320 mM sucrose) as well as in pure water. In water, however, the cubic phases were significantly more disordered compared to PBS and sucrose solutions (data not shown). In ×10 PBS the L_α–H_{II} transition temperatures were lowest in agreement with the known salt effects on the temperatures of the lipid phase transitions (39).

Regardless of their relatively good resolution, the ''powder'' diffraction patterns recorded in this work are not sufficient to distinguish between cubic phases within a given cubic aspect, e.g., to distinguish Pn3m from Pn3 (40,41). However, the assignments for these phases as Im3m and Pn3m phases are strongly supported by the circumstance that the cubic lattice parameter ratios are equal to 1.28 in all cases where the two cubic phases were found to coexist. The ratio of 1.28 has been calculated based on geometric considerations for the infinite periodic minimal surfaces underlying the inverse bicontinous cubic phases with Im3m and Pn3m symmetries (the Bonnet transformation) (42,43). As we invariably obtain 1.28 in all cases of coexisting cubic patterns, not only with DOPC/Chol systems but also with all other cubic phase dispersions that we have studied, we consider this fact a strong indication that the phases in question are indeed Im3m and Pn3m phases (see Tenchov et al. (33) for a more detailed discussion).

Dilinoleoyl PC/Chol 1:1 mixture in PBS was also found to convert readily into stable, long-lived cubic phase (Fig. 4 *A*). An $L_\alpha \rightarrow H_{II}$ transition occurred at ~80°C, and a single heating-cooling cycle through the latter transition was sufficient for full conversion into cubic phase. In contrast to DOPC/Chol mixtures, the cubic phase formed in this case was always a pure, well-ordered Pn3m cubic phase (Fig. 4 *A*). Also, we found that 1:1 mixtures with Chol of a saturated

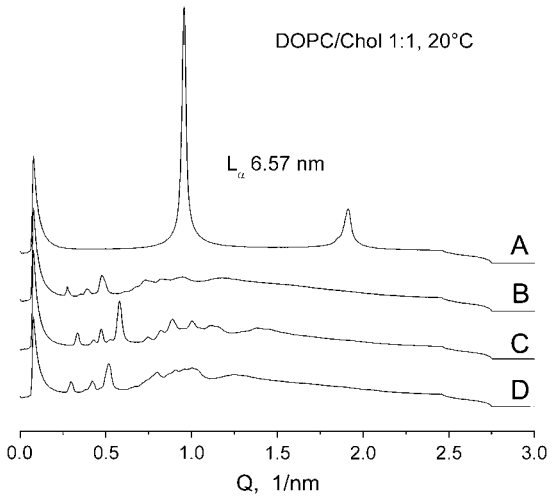

FIGURE 3 Phases in DOPC/Chol 1:1 mixtures, 10% (w/v) in PBS, at 20°C. (*A*) Initial lamellar phase L_α with spacing $d = 6.57$ nm. (*B—D*) Cubic phase patterns. (*B*) Im3m phase with lattice parameter of 32.3 nm obtained with the temperature protocol shown in Fig. 1 *B*. (*C*) Im3m phase (26.6 nm) with admixture of Pn3m phase (20.7 nm). (*D*) Im3m (30.1 nm) obtained after incubation at 76°C. No intensity adjustments have been made.

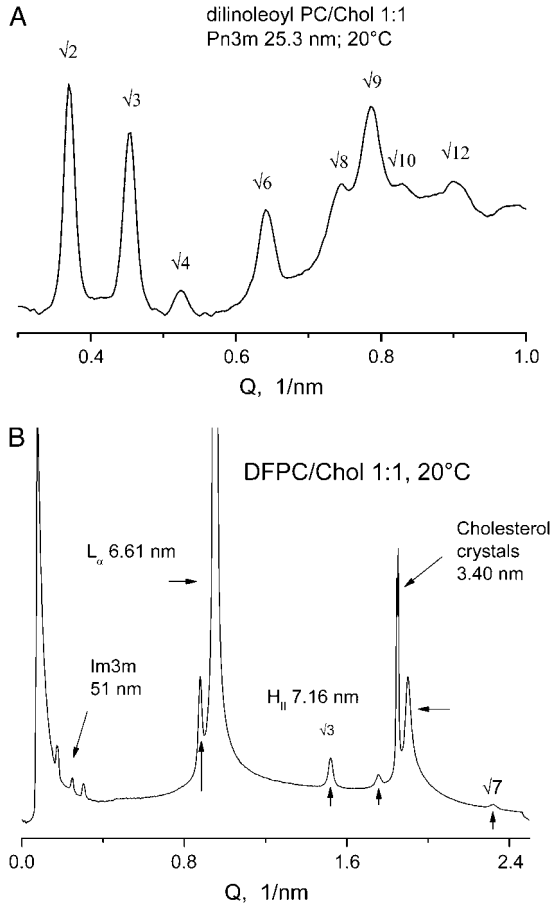

FIGURE 4 (*A*) Cubic Pn3m phase, lattice constant 25.3 nm, in dilinoleoyl PC/Chol 1:1 mixture, 10% (w/v) in PBS, after a heating-cooling cycle 20-98-20°C at 10°C/min ($L_\alpha \rightarrow H_{II} \rightarrow$ Pn3m). (*B*) Coexisting phases in diphytanoyl PC/Chol 1:1 mixture, 10% (w/v) in PBS, at 20°C (unheated preparation; see Materials and Methods).

branched-chain PC, diphytanoyl PC, can also form a cubic phase, albeit in a mixture with other phases (Fig. 4 *B*).

Unlike the mixtures of Chol with DOPC and dilinoleoyl PC, mixtures with Chol of two other unsaturated PCs, POPC and palmitoyl-linoleoyl PC, at 1:1 and 3:7 molar ratios did not display $L_\alpha \rightarrow H_{II}$ transitions in the accessible temperature range of up to ~95–100°C. No formation of stable cubic phases was observed in the latter mixtures, either. However, at PC/Chol molar ratio of 3:7, transient cubic traces appeared in both mixtures at ~90–95°C, although no H_{II} phase was evident in the x-ray patterns. These cubic traces disappeared on cooling to 75–80°C, giving way to fully recovered L_α phases (Fig. 5).

Role of the lipid concentration in the formation of DOPC/Chol cubic phases

In order to demonstrate the critical importance of using low lipid contents to facilitate the formation of cubic phases in PC/Chol mixtures, we also made measurements of DOPC/

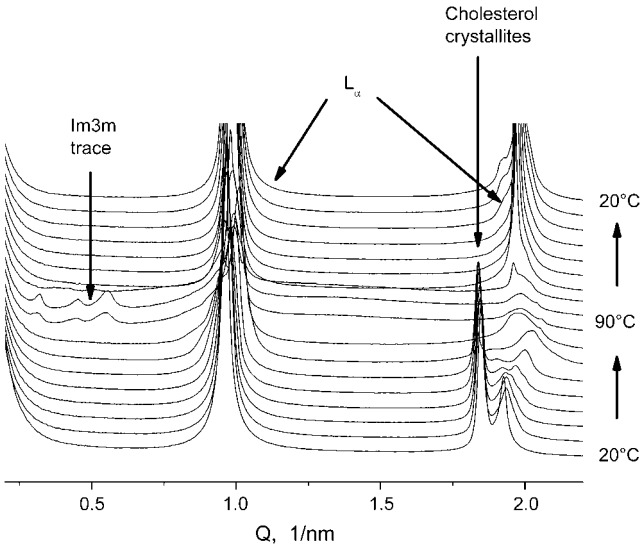

FIGURE 5 Transient cubic phase trace at high temperature in POPC/Chol 3:7 mixture, 10% (w/v) in PBS. Sequence of x-ray diffraction patterns recorded at every minute. Scan rate 10°C/min.

Chol 1:1 mixtures at higher lipid contents of 30% and 50% (w/v) using identical temperature protocols to ensure that the only variable in the series was an increasing lipid/water ratio. With the increase in lipid content, the conversion of the dispersions into cubic phase was strongly hindered, and the L_α phase was reformed to a much greater extent (Fig. 6). At 50% (w/v) of lipid, the L_α phase recovered almost completely, accompanied by a small contribution from the cubic phase. In addition, the type of cubic phase also changed with increasing lipid content, from pure Im3m or Im3m with Pn3m admixture at 10% (w/v) lipid (Fig. 6 *A*, also Fig. 3, *B–D*), to pure Pn3m cubic phase at 30% (w/v) (Fig. 6 *B*), and to the Ia3d (gyroid) cubic phase at 50% (w/v) of lipid (Fig. 6 *C*). The Ia3d phase was identified on basis of its two prominent $\sqrt{6}$ and $\sqrt{8}$ peaks and a range of overlapping, poorly resolved $\sqrt{14}$, $\sqrt{16}$, $\sqrt{20}$, $\sqrt{22}$, $\sqrt{24}$, and $\sqrt{26}$ reflections (Fig. 6 *B*, *inset*). As can be seen from Fig. 6 *A*, an Ia3d trace appears in the patterns at about the temperature of the reverse $H_{II} \rightarrow L_\alpha$ transition and persists on cooling to 20°C. It is clear from these measurements that, as an apparent manifestation of a restricted volume effect, high lipid contents suppress the development of the cubic phases and favor reformation of the L_α phase on cooling from the H_{II} phase range. The sequence Im3m → Pn3m → Ia3d observed with increase of the lipid content correlates with a decreasing water content of these three phases. Earlier we observed the same sequence for DEPE dispersions with increase of the DEPE content (see Tenchov et al. (33) for a discussion and related references). Another example of such a sequence is given by the phase diagram of lauric acid/dilauroyl PC 2:1 mixtures, which shows progressive formation of Im3d, Pn3m, and Ia3d with decreasing water content (44).

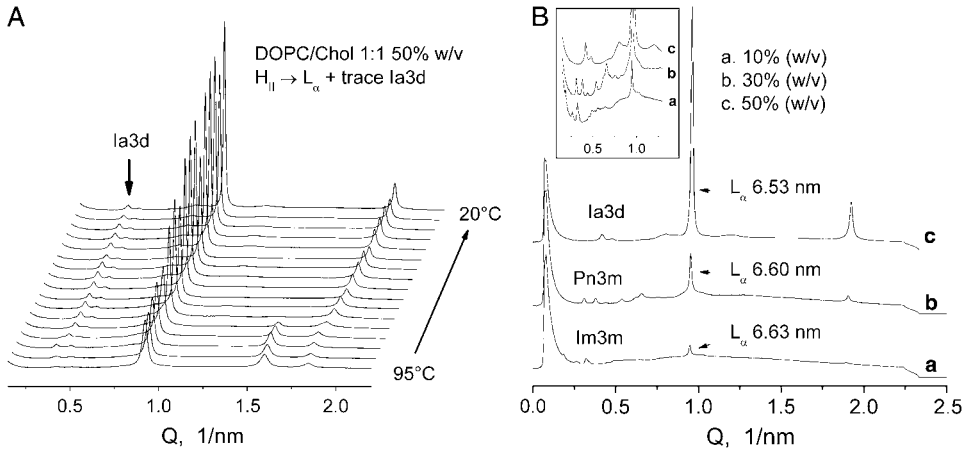

FIGURE 6 Supression of cubic phase formation in DOPC/Chol 1:1 mixtures by increase of the lipid/water ratio. (*A*) Cooling scan of a DOPC/Chol 1:1 mixture, 50% (w/v) in PBS, showing almost complete recovery of the L_α phase from the H_{II} phase, accompanied by a small amount of Ia3d cubic phase. Scan rate 5°C/min. (*B*) Effect of the lipid content on the cubic phase formation in DOPC/Chol 1:1 mixtures in PBS. Diffraction patterns recorded at 20°C after a heating-cooling scan 20-95-20°C: (*a*) 10% (w/v), Im3m 48.0 nm; (*b*) 30% (w/v), Pn3m 28.8 nm; (*c*) 50% (w/v), Ia3d 36.8 nm.

Role of the PC/Chol molar ratio

On the basis of our measurements, the DOPC/Chol molar ratio of 1:1 appears to be close to the maximum possible uptake of Chol by DOPC membranes. A clear indication that the saturation level has been exceeded is the appearance of diffraction lines or spots in the x-ray patterns arising from excess, phase-separated crystalline Chol. The presence of Chol crystallites is particularly well discernible in the 2-D patterns, where they are manifested as a spotty diffraction line with 3.40-nm spacing (Fig. 7 *A*). They are also visible, albeit less clearly, in the axially integrated 1-D patterns (Fig. 7 *B*). Although some of our 1:1 preparations displayed trace amounts of Chol crystals in the initial L_α phase, other preparations, both in the same and in different sample series, did not, indicating that the saturation level is actually within the error limits of our DOPC/Chol (1:1) preparations. These observations are consistent with the DSC results of Epand et al. (30), which show that the excess Chol limit for DOPC is between 0.5 and 0.6 Chol molar fraction. Whenever present, the excess Chol traces diminished on heating of the samples and were completely absent from the 2-D patterns of the H_{II} and cubic phases. It appears that Chol uptake by DOPC increases with temperature, enhancing the tendency for inverted phase formation at high temperatures, and also that the H_{II} and the cubic phases have higher Chol saturation levels relative to the L_α phase.

As expected, DOPC/Chol 3:7 mixtures displayed a high level of excess Chol. This is evident from the large number of Chol crystallite spots, which form almost smooth diffraction rings in the 2-D patterns (*not shown*). The 3:7 mixtures also displayed a facile conversion into cubic phases with characteristics similar to those for the process of cubic phase formation in 1:1 mixtures. However, the excess Chol remained well visible in the patterns in all phases and at all temperatures, and the diffraction patterns of the cubic phases so formed were typified by broader, more poorly resolved reflections than 1:1 mixtures. A possible reason for the diminished resolution in 3:7 mixtures could be the higher concentration of Chol crystallites, which may serve to hinder the formation of large, well-correlated liquid crystalline domains.

Diphytanoyl PC (DFPC) appears to have a Chol saturation level that is lower than that of DOPC. This is evident from Fig. 4 *B*, which shows the intial unheated state of a DFPC/Chol 1:1 mixture, in which there is a large peak of excess crystalline Chol in addition to peaks corresponding to a mixture of the L_α, H_{II}, and cubic Im3m phases. The L_α–H_{II} phase transition in the 1:1 DFPC/Chol mixture is obviously below room temperature, and it would appear that better conditions for cubic phase formation could be found at Chol fractions of <0.5.

DISCUSSION

New role of Chol: Chol as membrane "fusogen"

In this work we present direct evidence from x-ray diffraction that Chol, a major and ubiquitous biomembrane component,

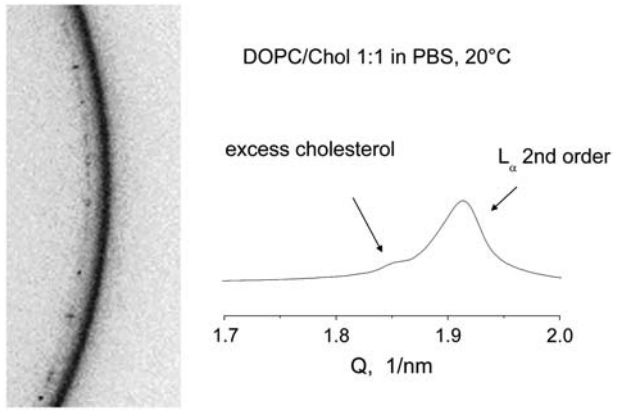

FIGURE 7 Diffraction from excess Chol crystallites in the L_α phase of a DOPC/Chol 1:1 mixture, 10% (w/v) in PBS, 20°C. (*A*) Cutoff from a 2-D diffraction pattern. (*B*) Axially integrated 1-D pattern obtained from the 2-D pattern in *A*.

induces formation of inverted bicontinuous cubic phases in mixtures with unsaturated PCs. This is a new, previously undescribed effect of Chol that may have important implications for its biological functions, in particular, for its role in viral fusion. The PCs are the major phospholipid class in biological membranes, and, in contrast with the PEs, the membrane PCs are nonfusogenic lipids. They cannot form inverted phases by themselves, whereas an inverted phase–forming ability is correlated with susceptibility to membrane fusion (45). It is thus of clear interest that mixtures of unsaturated PCs with another major membrane lipid, Chol, can readily transform into an inverted bicontinuous cubic phase. This finding certainly reduces and illuminates in a new way the requirements for the presence of fusogenic, inverted-phase-forming lipids that are able to render a membrane fusogenic. Because the formation of bicontinuous inverted cubic phases is closely correlated with lipid membrane fusogenicity (46), our results imply that a membrane need not have large amounts of PE to be fusogenic; alternatively, high concentrations of Chol like those found in plasma membranes can render a fusion-refractory lipid fusogenic. This is compatible with the effects of Chol on viral fusion (14–26) and with the reported requirement of Chol for fast and efficient fusion of sea urchin cortical granule fusion and exocytosis (27).

Basic properties of the cubic phases in PC/Chol mixtures

Cubic phase formation in PC/Chol mixtures displayed a number of features that are very similar to those observed previously for PE dispersions (33). For both kinds of dispersions, the cubic phases are closely associated with the L_α–H_{II} transition, and their formation is most easily induced by cooling the H_{II} phase. Another common property of the PE and PC/Chol cubic phases is that their formation is accelerated and can proceed to completion in sufficiently diluted lipid dispersions only. Because of their specific geometric structure, the inverted bicontinuous cubic spaces require aqueous volumes for their development that are much larger than the so-called excess water limit required for full hydration of the lipid polar groups (see Tenchov et al. (33) for a discussion). In our study, we recorded a facile, near-complete conversion of the lamellar phase into a cubic phase after a single heating-cooling cycle through the $L_\alpha \leftrightarrow H_{II}$ phase transition of DOPC/Chol and dilinoleoyl PC/Chol mixtures at lipid content of 10% (w/v) (Figs. 1–4). Increasing the lipid content resulted in hindered transformation into cubic phase and favored reformation of the initial lamellar phase during cooling from the H_{II} phase range (Fig. 6).

Similarly to the PEs, the PC/Chol mixtures are able to form all three kinds of inverted bicontinuous phases, Im3m, Pn3m, and Ia3d, depending on the lipid content in the dispersion (Fig. 6). In those cases where the Im3m and Pn3m phases were found to coexist, their lattice constant ratio was exactly 1.28, as expected from geometric consideratiions for coexisting phases of this type (42,43). With increasing lipid content from 10% to 50% (w/v), the DOPC/Chol 1:1 mixtures displayed a cubic phase sequence Im3m → Pn3m → Ia3d, consistent with a decreasing water content of these three phases. As noted by Templer et al. (44), this sequence appears to be universal, although not all three inverse bicontinuous cubic phases should necessarily appear in a given system.

In contrast to the DOPC/Chol and dilinoleoyl PC/Chol mixtures, mixtures of Chol with POPC and palmitoyl-oleoyl PC only transiently entered cubic phases at high temperatures (~90°C and above) and even then, only in PC/Chol 3:7 mixtures, and not in 1:1 mixtures (Fig. 5). The reason for the strong effect of the PC acyl chain composition on cubic phase formation is obviously associated with the different temperature ranges of the L_α–H_{II} transition in different PC/Chol mixtures. We did not observe formation of H_{II} phases for mixtures of Chol with POPC and palmitoyl-linoleoyl PC up to 95–100°C, and we conclude that their L_α–H_{II} transition ranges, within which a cubic phase could form, are located at even higher temperatures.

The cubic phases formed in DOPC/Chol and dilinoleoyl PC/Chol mixtures were able to supercool and hence to supplant the initial L_α phase at low temperatures. Although these phases form only at high temperatures, once formed they remain stable over a broad range of physiological temperatures. In particular, their structures do not change, and no lamellar phase reappears on storage for up to at least 6–10 h at room temperature.

Potential dual role for Chol in fusion and raft formation

In ternary mixtures, saturated PCs and SM are known to separate, along with Chol, into liquid-ordered domains. Our results suggest that unsaturated PCs, which are excluded from these domains, could form fusogenic domains with Chol. Such dual effects of Chol may explain the seemingly paradoxical ability of cell membranes to simultaneously form rigid, low-curvature ''raft''-like patches, while still being able to undergo facile membrane fusion, as in exocytosis, endocytosis, and viral infection.

Chol is, in essence, a planar molecule that can interact hydrophobically on both surfaces. The tetracyclic ring structure is rigid, and the location of the hydroxyl group dictates the predominant orientation of the molecule in a membrane bilayer. Although this structure apparently favors a more compact chain packing and formation of liquid-ordered domains, it is clear from previous studies on the formation of inverted hexagonal phase, H_{II} (30–32), as well as from the present results on formation of inverted cubic phases that Chol also promotes both H_{II} and cubic phases in unsaturated PCs at appropriately high concentrations and temperatures. It is known that Chol increases the negative spontaneous

curvature of DOPC (29), a trend that favors inverted phase formation. From data in Chen and Rand (29), the spontaneous radius of curvature of a DOPC/Chol 1:1 mixture at 32°C is expected to be approximately −4 nm, close to the values observed in PE H_{II} phases (approximately −3 nm). The curvature becomes more negative with increasing temperature, so inverted phases will be even more favored at temperatures above 60–70°C, where we observed spontaneous inverted cubic phase formation. Chol has the unique characteristic among membrane lipids of rapidly flip-flopping, and because of its small head, a negative curvature is made easier by an accumulation of Chol. This facilitates bending, an essential characteristic for cell membranes, but especially for those that are in communication with the cell surface membrane. The latter membranes are those that also contain the bulk of the cell's Chol.

There is increasing experimental evidence for the existence of domains of ordered lipids in biomembranes, although these domains may only be on the order of 100 nm in size (47–51). The ordered domains may play important roles in signal transduction, endocytosis, exocytosis, viral infection, and other functions (24,52–55). For example, the domains may spatially organize the proteins involved in controlling or mediating membrane fusion, as discussed by Churchward et al. (27). It has been suggested that segregation of the more unsaturated-chain PCs within biomembranes could have physiological implications. One of those implications could be for local modification of the fusogenicity of the membrane lipids. Formation of liquid ordered domains automatically enriches other regions of the membrane in unsaturated PCs. Control of the extent of lateral phase separation of unsaturated PCs may be one mechanism that cells use to control the spatial and temporal occurrence of fusion events.

This work was supported by National Institutes of Health (NIH) GM 57305. Synchrotron x-ray measurements were performed at DND-CAT and BioCAT at APS, Argonne National Laboratory. BioCAT is NIH-supported, Grant RR08630. DND-CAT is supported by E. I. DuPont de Nemours & Co., The Dow Chemical Company, National Science Foundation Grant DMR-9304725, and the state of Illinois through the Dept. of Commerce and the Board of Higher Education Grant IBHE HECA NWU 96. Use of APS was supported by the U.S. Department of Energy, Basic Energy Sciences, Office of Energy Research, Contract No. W-31-102-Eng-38.

REFERENCES

1. Finegold, L. 1993. Cholesterol in Membrane Models. CRC Press, Ann Arbor, MI.
2. Ladbrook, B. D., R. M. Williams, and D. Chapman. 1968. Studies on lecithin-cholesterol-water interactions by differential scanning calorimetry and x-ray diffraction. *Biochim. Biophys. Acta.* 150:333–340.
3. Ipsen, J. H., G. Karlstrom, O. G. Mouritsen, H. Wennerstrom, and M. J. Zuckermann. 1987. Phase-equilibria in the phosphatidylcholine-cholesterol system. *Biochim. Biophys. Acta.* 905:162–172.
4. Ohvo-Rekila, H., B. Ramstedt, P. Leppimaki, and J. P. Slotte. 2002. Cholesterol interactions with phospholipids in membranes. *Prog. Lipid Res.* 41:66–97.
5. van Duyl, B. Y., D. Ganchev, V. Chupin, B. de Kruijff, and J. A. Killian. 2003. Sphingomyelin is much more effective than saturated phosphatidylcholine in excluding unsaturated phosphatidylcholine from domains formed with cholesterol. *FEBS Lett.* 547:101–106.
6. Shaikh, S. R., A. C. Dumaual, A. Castillo, D. LoCascio, R. A. Siddiqui, W. Stillwell, and S. R. Wassall. 2004. Oleic and docosahexaenoic acid differentially phase separate from lipid raft molecules: A comparative NMR, DSC, AFM, and detergent extraction study. *Biophys. J.* 87:1752–1766.
7. Wassall, S. R., M. R. Brzustowicz, S. R. Shaikh, V. Cherezov, M. Caffrey, and W. Stillwell. 2004. Order from disorder, corralling cholesterol with chaotic lipids—The role of polyunsaturated lipids in membrane raft formation. *Chem. Phys. Lipids.* 132:79–88.
8. de Almeida, R. F. M., A. Fedorov, and M. Prieto. 2003. Sphingomyelin/phosphatidylcholine/cholesterol phase diagram: Boundaries and composition of lipid rafts. *Biophys. J.* 85:2406–2416.
9. Veatch, S. L., I. V. Polozov, K. Gawrisch, and S. L. Keller. 2004. Liquid domains in vesicles investigated by NMR and fluorescence microscopy. *Biophys. J.* 86:2910–2922.
10. Crane, J. M., and L. K. Tamm. 2004. Role of cholesterol in the formation and nature of lipid rafts in planar and spherical model membranes. *Biophys. J.* 86:2965–2979.
11. Brown, D. A., and E. London. 1998. Functions of lipid rafts in biological membranes. *Annu. Rev. Cell Dev. Biol.* 14:111–136.
12. Brown, D. 2002. Structure and function of membrane rafts. *Int. J. Med. Microbiol.* 291:433–437.
13. Lucero, H. A., and P. W. Robbins. 2004. Lipid rafts-protein association and the regulation of protein activity. *Arch. Biochem. Biophys.* 426: 208–224.
14. Wilschut, J., J. Corver, J. L. Nieva, R. Bron, L. Moesby, K. C. Reddy, and R. Bittman. 1995. Fusion of Semliki-Forest-virus with cholesterol-containing liposomes at low pH—a specific requirement for sphingolipids. *Mol. Membr. Biol.* 12:143–149.
15. Nieva, J. L., R. Bron, J. Corver, and J. Wilschut. 1994. Membrane-fusion of Semliki Forest virus requires sphingolipids in the target membrane. *EMBO J.* 13:2797–2804.
16. Waarts, B. L., R. Bittman, and J. Wilschut. 2002. Sphingolipid and cholesterol dependence of alphavirus membrane fusion—Lack of correlation with lipid raft formation in target liposomes. *J. Biol. Chem.* 277: 38141–38147.
17. Lu, Y. P. E., T. Cassese, and M. Kielian. 1999. The cholesterol requirement for Sindbis virus entry and exit and characterization of a spike protein region involved in cholesterol dependence. *J. Virol.* 73:4272–4278.
18. Smit, J. M., R. Bittman, and J. Wilschut. 1999. Low-pH-dependent fusion of sindbis virus with receptor-free cholesterol- and sphingolipid-containing liposomes. *J. Virol.* 73:8476–8484.
19. Saez-Cirion, A., S. Nir, M. Lorizate, A. Agirre, A. Cruz, J. Perez-Gil, and J. L. Nieva. 2002. Sphingomyelin and cholesterol promote HIV-1 gp41 pretransmembrane sequence surface aggregation and membrane restructuring. *J. Biol. Chem.* 277:21776–21785.
20. Liao, Z. H., L. M. Cimakasky, R. Hampton, D. H. Nguyen, and J. E. K. Hildreth. 2001. Lipid rafts and HIV pathogenesis: Host membrane cholesterol is required for infection by HIV type 1. *AIDS Res. Hum. Retroviruses.* 17:1009–1019.
21. Liao, Z. H., D. R. Graham, and J. E. K. Hildreth. 2003. Lipid rafts and HIV pathogenesis: Virion-associated cholesterol is required for fusion and infection of susceptible cells. *AIDS Res. Hum. Retroviruses.* 19:675–687.
22. Viard, M., I. Parolini, M. Sargiacomo, K. Fecchi, C. Ramoni, S. Ablan, F. W. Ruscetti, J. M. Wang, and R. Blumenthal. 2002. Role of cholesterol in human immunodeficiency virus type 1 envelope protein-mediated fusion with host cells. *J. Virol.* 76:11584–11595.
23. Vincent, N., C. Genin, and E. Malvoisin. 2002. Identification of a conserved domain of the HIV-1 transmembrane protein gp41 which interacts with cholesteryl groups. *Biochim. Biophy. Acta.* 1567: 157–164.

24. Rawat, S. S., M. Viard, S. A. Gallo, A. Rein, R. Blumenthal, and A. Puri. 2003. Modulation of entry of enveloped viruses by cholesterol and sphingolipids (Review). *Mol. Membr. Biol.* 20:243–254.
25. Sun, X. J., and G. R. Whittaker. 2003. Role for influenza virus envelope cholesterol in virus entry and infection. *J. Virol.* 77:12543–12551.
26. Shnaper, S., K. Sackett, S. A. Gallo, R. Blumenthal, and Y. Shai. 2004. The C- and the N-terminal regions of glycoprotein 41 ectodomain fuse membranes enriched and not enriched with cholesterol, respectively. *J. Biol. Chem.* 279:18526–18534.
27. Churchward, M. A., T. Rogasevskaia, J. Hofgen, J. Bau, and J. R. Coorssen. 2005. Cholesterol facilitates the native mechanism of Ca^{2+}-triggered membrane fusion. *J. Cell Sci.* 118:4833–4848.
28. Dimitrov, D. S. 2004. Virus entry: Molecular mechanisms and biomedical applications. *Nat. Rev. Microbiol.* 2:109–122.
29. Chen, Z., and R. P. Rand. 1997. The influence of cholesterol on phospholipid membrane curvature and bending elasticity. *Biophys. J.* 73:267–276.
30. Epand, R. M., D. W. Hughes, B. G. Sayer, N. Borochov, D. Bach, and E. Wachtel. 2003. Novel properties of cholesterol-dioleoylphosphatidylcholine mixtures. *Biochim. Biophy. Acta.* 1616:196–208.
31. Epand, R. M., R. F. Epand, A. D. Bain, B. G. Sayer, and D. W. Hughes. 2004. Properties of polyunsaturated phosphatidylcholine membranes in the presence and absence of cholesterol. *Magn. Reson. Chem.* 42:139–147.
32. Epand, R. M., R. F. Epand, D. W. Hughes, B. G. Sayer, N. Borochov, D. Bach, and E. Wachtel. 2005. Phosphatidylcholine structure determines cholesterol solubility and lipid polymorphism. *Chem. Phys. Lipids.* 135:39–53.
33. Tenchov, B., R. Koynova, and G. Rapp. 1998. Accelerated formation of cubic phases in phosphatidylethanolamine dispersions. *Biophys. J.* 75:853–866.
34. Tenchov, B., R. C. MacDonald, and D. P. Siegel. 2005. Inverted bicontinuous cubic phases in unsaturated PC/cholesterol mixtures: A dual role for cholesterol in fusion and raft formation? *Biophys. J.* 88:68A. (Abstr.)
35. Toombes, G. E. S., A. C. Finnefrock, M. W. Tate, and S. M. Gruner. 2002. Determination of L-alpha-H-II phase transition temperature for 1,2-dioleoyl-*sn*-glycero-3-phosphatidylethanolamine. *Biophys. J.* 82: 2504–2510.
36. Tenchov, B., M. Rappolt, R. Koynova, and G. Rapp. 1996. New phases induced by sucrose in saturated phosphatidylethanolamines: An expanded lamellar gel phase and a cubic phase. *Biochim. Biophy. Acta.* 1285:109–122.
37. Siegel, D. P., and J. L. Banschbach. 1990. Lamellar inverted cubic (L-alpha Qii) phase-transition in N-methylated dioleoylphosphatidylethanolamine. *Biochemistry.* 29:5975–5981.
38. Kasper, J. S., and K. Lonsdale, editors. 1985. International Tables for X-Ray Crystallography, Vol. 2 D. Riedel Publishing, Dordrecht, The Netherlands.
39. Koynova, R., J. Brankov, and B. Tenchov. 1997. Modulation of lipid phase behavior by kosmotropic and chaotropic solutes - Experiment and thermodynamic theory. *Eur. Biophys. J. Biophy.* 25:261–274.
40. Longley, W., and T. J. McIntosh. 1983. A bicontinuous tetrahedral structure in a liquid-crystalline lipid. *Nature.* 303:612–614.
41. Harper, P. E., and S. M. Gruner. 2000. Electron density modeling and reconstruction of infinite periodic minimal surfaces (IPMS) based phases in lipid-water systems. I. Modeling IPMS-based phases. *Eur. Phys. J. E.* 2:217–228.
42. Andersson, S., S. T. Hyde, K. Larsson, and S. Lidin. 1988. Minimal-surfaces and structures—from inorganic and metal crystals to cell-membranes and bio-polymers. *Chem. Rev.* 88:221–242.
43. Hyde, S. T., S. Andersson, B. Ericsson, and K. Larsson. 1984. A cubic structure consisting of a lipid bilayer forming an infinite periodic minimum surface of the gyroid type in the glycerolmonooleate-water system. *Z. Kristallogr.* 168:213–219.
44. Templer, R. H., J. M. Seddon, N. A. Warrender, A. Syrykh, Z. Huang, R. Winter, and J. Erbes. 1998. Inverse bicontinuous cubic phases in 2:1 fatty acid phosphatidylcholine mixtures. The effects of chain length, hydration, and temperature. *J. Phys. Chem. B.* 102:7251–7261.
45. Siegel, D. P. 2005. Lipid membrane fusion. *In* The Structure of Biological Membranes, 2nd edition. P.L.Yeagle, editor. CRC Press, Boca Raton, FL. 255–308.
46. Siegel, D. P. 2005. Relationship between bicontinuous inverted cubic phases and membrane fusion. *In* Bicontinuous Liquid Crystals, Surfactant Science Series, Vol. 127. M. L. Lynch and P. T. Spicer, editors. Marcel Dekker, New York.
47. Edidin, M. 2003. The state of lipid rafts: From model membranes to cells. *Annu. Rev. Biophys. Biomol. Struct.* 32:257–283.
48. McMullen, T. P. W., R. N. A. H. Lewis, and R. N. McElhaney. 2004. Cholesterol-phospholipid interactions, the liquid-ordered phase and lipid rafts in model and biological membranes. *Curr. Opin. Colloid In.* 8:459–468.
49. Simons, K., and W. L. C. Vaz. 2004. Model systems, lipid rafts, and cell membranes. *Annu. Rev. Biophys. Biomol. Struct.* 33:269–295.
50. Laude, A. J., and I. A. Prior. 2004. Plasma membrane microdomains: organization, function and trafficking (Review). *Mol. Membr. Biol.* 21:193–205.
51. Mayor, S., and M. Rao. 2004. Rafts: Scale-dependent, active lipid organization at the cell surface. *Traffic.* 5:231–240.
52. Salaun, C., D. J. James, and L. H. Chamberlain. 2004. Lipid rafts and the regulation of exocytosis. *Traffic.* 5:255–264.
53. Helms, J. B., and C. Zurzolo. 2004. Lipids as targeting signals: Lipid rafts and intracellular trafficking. *Traffic.* 5:247–254.
54. Golub, T., S. Wacha, and P. Caroni. 2004. Spatial and temporal control of signaling through lipid rafts. *Curr. Opin. Neurobiol.* 14:542–550.
55. Devaux, P. F., and R. Morris. 2004. Transmembrane asymmetry and lateral domains in biological membranes. *Traffic.* 5:241–246.